Published in final edited form as:
Microbes Infect. 2009 December ; 11(14-15): 1140–1149. doi:10.1016/j.micinf.2009.08.009.

Transcriptomic alterations in *Trypanosoma cruzi*-infected cardiac myocytes

Regina Coeli dos Santos Goldenberg[a,b,c], **Dumitru A. Iacobas**[b], **Sanda Iacobas**[b], **Leonardo Lima Rocha**[a,1], **Fabio da Silva de Azevedo Fortes**[a,b,c], **Leandro Vairo**[a,c], **Fnu Nagajyothi**[a], **Antonio Carlos Campos de Carvalho**[b,c], **Herbert B. Tanowitz**[a], and **David C. Spray**[b,*]

[a] Department of Pathology, Albert Einstein College of Medicine, Bronx, NY, USA

[b] Dominick P Purpura Department of Neuroscience, Albert Einstein College of Medicine, Bronx, NY 10461, USA

[c] Instituto de Biofísica Carlos Chagas Filho, Universidade Federal do Rio de Janeiro, Rio de Janeiro, Brazil

Abstract

Trypanosoma cruzi infection is a major cause of cardiomyopathy. Previous gene profiling studies of infected mouse hearts have revealed prominent changes in gene expression within many functional pathways. This variety of transcriptomic changes in infected mice raises the question of whether gene expression alterations in whole hearts are due to changes in infected cardiac myocytes or other cells or even to systemic effects of the infection on the heart. We employed microarrays to examine infected cardiac myocyte cultures 48 h post-infection. Statistical comparison of gene expression levels of 7624 well annotated unigenes in four independent cultures of infected and uninfected myocytes detected substantial (≥1.5 absolute fold changes) in 420 (5.5%) of the sampled genes. Major categories of affected genes included those involved in immune response, extracellular matrix and cell adhesion. These findings on infected cardiac myocytes in culture reveal that alterations in cardiac gene expression described in Chagas disease are the consequence of both direct infection of the myocytes themselves as well as resulting from the presence of other cell types in the myocardium and systemic effects of infection.

Keywords

Trypanosoma cruzi; Chagas disease; Microarray; Cardiomyopathy; Cardiac myocyte culture

1. Introduction

Chagas' disease or American Trypanosomiasis is caused by infection with the protozoan parasite, *Trypanosoma cruzi*. Infection with this parasite causes both an acute myocarditis as well as chronic dilated cardiomyopathy [1]. It is estimated that 15–30 percent of infected individuals develop chronic chagasic cardiomyopathy, which is manifested by conduction disturbances, thrombo-embolic events and congestive heart failure [1]. Blood form trypomastigotes are capable of infecting many cell types in the cardiovascular system, including endothelial and smooth muscle cells, fibroblasts and cardiac myocytes [1]. The

*Correspondence to: David C. Spray, Dominick P. Purpura Department of Neuroscience, Room 840 Kennedy Center, Albert Einstein College of Medicine, 1410 Pelham Parkway So, Bronx, NY 10461, USA. Tel.: +1 718 430 2537; fax: +1 718 430 8594. spray@aecom.yu.edu (D.C. Spray).
[1]Present address: Department of Cardiothoracic Surgery, University of Sao Paulo, Sao Paulo, Brazil.

parasites gain access to cardiac myocytes by first invading the endothelium and then traversing the interstitial areas of the vascular and myocardial wall. Trypomastigotes also traverse the basal laminae areas and the extracellular matrix, which is damaged as a result of parasite proteases and collagenases and by contributions from the host inflammatory response [1]. There then ensues cardiovascular remodeling and replacement of cardiac myocytes and vascular cells by fibrous tissue. This results in thinning of the myocardium and cardiac myocyte hypertrophy and myocardial dysfunction. Importantly, the parasitism of host cells in the cardiovascular system activates a variety of host cell signaling pathways [2–4].

The study of chagasic heart disease has been aided by the use of the mouse model which recapitulates many of the functional and pathological alterations of the human disease. In the myocardium of acutely infected mice, the inflammatory reaction is characterized by the presence of numerous parasite pseudocysts together with an intense inflammatory reaction and an increased expression of inflammatory mediators as well as components of the endothelin-1 pathway [2].

Gene expression microarrays provide a powerful technique to profile genome-wide levels of thousands of mRNA transcripts simultaneously. Microarray technology has been applied in the identification of genes that are altered in infected cells [5,6] and in the hearts of *T. cruzi* infected mice and in human specimens [7–10]. However, microarray analysis of the whole heart detects the sum of changes in many cell types. Because cardiac myocytes themselves are important targets of initial infection, we used primary cultures of cardiac myocytes to examine gene profiling of *T. cruzi*-infected cardiac myocytes. In this way we could examine the effect of infection on cardiac myocytes devoid of any contribution of other cells in the myocardium or of systemic effects of infection. Our findings indicate substanitally altered expression of more than 5% of the sampled genome with major alterations in genes related to inflammation, immunological responses and cell adhesion. Thus, the inflammatory consequences of myocyte infection in the heart result not only from immunological response of the whole heart but also through induction of endogenous pathways in the myocyte. Moreover, patterns of altered genes include those encoding junction-associated proteins that are frequent genetic targets leading to cardiomyopathy.

2. Materials and methods

2.1. Preparation of primary cultures of cardiac myocytes

Neonatal mice (C57BL/6, Charles River Laboratories, Wilmington, MA) were killed by decapitation, and the hearts were isolated and placed in 60 mm plastic culture dishes containing sterile ice-cold Dulbecco's phosphate-buffered saline (PBS; GIBCO-BRL, Grand Island, NY). After rinsing with PBS to remove the blood, we thoroughly minced the hearts in the dissociation solution [containing 1.25% pancreatin (GIBCO-BRL) and 300 mg/L bovine serum albumin (BSA; Sigma, St. Louis, MO) diluted in (in g/L) 8.0 NaCl, 0.2 KCl, 0.05 Na_2HPO_4, 1.0 $NaHCO_3$, and 2.0 dextrose; [pH 7.1–7.2]. The homogenate was then transferred to a 25 ml Ehrlenmeyer flask with 7 ml of the dissociation solution and placed in a water bath (37 °C) for 10 min while continuously stirring. The supernatant fraction containing single cells from each digestion period was collected in a conical 15 ml tube and spun at 500 g for 4 min, and the pellet was re-suspended in 3 ml of Dulbecco's modified Eagle's medium (DMEM) [containing 10% fetal bovine serum (GIBCO-BRL) and 1% penicillin/streptomycin (GIBCO-BRL)]. The tube with the dissociated cells was then placed in the incubator (37 °C, 5% CO_2). This procedure was repeated five to seven times or until the heart tissue was totally dissociated. The cells were pooled and preplated, in 100 mm plastic culture dishes for 1 h, to allow the non muscle cells to attach. Then, the remaining unattached cells, highly enriched in myocytes, were plated (2×10^5 cells/cm^2) into 12.5 cm^2 plastic culture flasks (Falcon, USA), placed in the incubator, and allowed to settle for 24 h. After this period, we washed the flasks with DMEM to remove the

non-adherent cells and fed the cells with 3 ml of DMEM supplemented with cytosine β-D-arabino-furanoside (12.2 mg/50 ml media; Sigma) to inhibit fibroblast growth. The cultures were maintained at 37 °C in a 5% CO_2 humidified incubator. All animal protocols were approved by our institutional animal care and use committee.

2.2. Infection of the cultures

Four days after the cardiac myocytes were plated, they displayed spontaneous contractility; based upon morphology and fraction of contractile cells, purity of cultures was estimated to be 85–90%, with the remainder being fibroblasts and endothelial cells. Cutlures were then infected with trypomastigotes of the myotropic Brazil strain of *T. cruzi* at a multiplicity of infection of 5:1. Parasites were maintained and harvested from L_6E_9 myoblasts as previously described [11]. After 24 h of incubation, the cultures were washed thoroughly with medium and maintained as described above. At 48 h after infection the percent parasitism was determined by staining replicate dishes in situ with May–Grunwald–Giemsa [12]. The percent parasitism was approximately 75% at the time when the cells were harvested for microarray analysis.

2.3. RNA analysis

Total RNA was extracted in Trizol® according to an established, standardized protocol from four dishes of control (C1, C2, C3, C4) and four infected cultures of cardiac myocytes (I1, I2, I3, I4) to ensure statistical relevance of the study. 3 μg total RNA from each control or infected cell culture was amplified in a single round protocol using Ambion® Amino Allyl MessageAmp™ II aRNA Amplification kit (http://www.ambion.com/techlib/resources/messageamp/chart.html) to obtain 10 μg Alexa Fluor®_555-labeled (green, g) cDNA or Alexa Fluor®_647-labeled (red, r)cDNAs. Differently labeled biological replicas were then co-hybridized with microarrays printed by the Albert Einstein College of Medicine Microarray Facility with 32k mouse 70-mer oligonucleotides (Operon v.3.0, full technical information in GPL5371). Four microarrays were hybridized overnight at 50 °C with the combinations: C1(r)C2(g), C3(r)C4(g), I1(r)I2(g), I3(r)I4(g) (“multiple yellow” design, [13]). After hybridization, the slides were washed at room temperature, in solutions containing 0.1% sodium dodecyl sulfate (SDS) and 1% SSC (3 M NaCl + 0.3 M sodium citrate) to remove the nonhybridized cDNAs. Slides were immediately scanned, with the same pair of accelerating voltages in the two channels: 600 V(r) and 540 V (g).

The images were acquired and initially analyzed with GenePix Pro 4.1 software. Raw data were further normalized and mined through in-house-developed algorithms that incorporate standard procedures [13,14]. Locally corrupted or saturated spots, as well as those for which the foreground median fluorescence did not exceed twice the median local background fluorescence in one sample were eliminated from the analysis in all samples. The net fluorescence, i.e. the background subtracted from the foreground signal, of each validated spot was transformed through intra- and inter-chip normalization, aiming to obtain biologically meaningful comparisons between the studied specimens. Intrachip normalization balances the averages of net fluorescence values in the two channels within each pin domain (subset of spots printed by the same pin), corrects the intensity-dependent bias (usually referred to as Lowess normalization), and forces the standard distribution (mean 0 and standard deviation 1) of $\log_2$ ratios (scale normalization) of net fluorescent values in the two channels for each array. Inter-chip normalization assigns a ratio between the corrected net fluorescence of each valid spot and the average net fluorescence of all valid spots in both control (C1, C2, C3, C4) and experimental (11, I2, I3, I4) arrays. The spots probing the same gene were organized into redundancy groups and their background subtracted fluorescence replaced by a weighted average value.

2.4. Real time PCR determinations

For real time PCR (qPCR) determinations RNA was isolated from infected myocytes using the Trizol reagent following the manufacturer's protocol (Invitrogen, Carlsbad, CA). RNA was reverse-transcribed from 100 ng of total RNA in a final volume of 20 μl using Superscript II reverse transcriptase according to the manufacturer's protocol (Invitrogen, Carlsbad, CA). The reverse transcription mixture consisted of 0.5 mM dNTPs, 20 mM dithiothritol, 30 mM Tris HCl pH 8.3, 75 mM KCl, 3 mM MgCl2, 500 ng oligo dT and 200 U of superscript RT RNase H-reverse transcriptase (Invitrogen). The reaction was incubated for 50 min at 42 °C. The primers used for amplification of qPCR were as follows:

Aquaporin-1 (269 bp)

Aqp Forward: CAATTACCCACTGGAGGAGAAAC

Aqp Reverse: CAAGTGAATTGTCGACTAGGG

Profilin-1 (202 bp)

Pfn Forward: GGAAGACCTTCGTTAGCATTAC

Pfn Reverse: GTGACAGTGACATTGAA

MMP12 (267 bp)

Mmp12 Forward: ACAACTTAGTACCAGAGCCACAC

Mmp12 Reverse: CTCCTTGGAAGATGTAGTAGTGTC

Bst2 (138 bp)

Bst2 Forward: AGGAGCTTGAGAATGAAGTCAC

Bst2 Reverse: GTGACACTTTGAGCACCAGTAG

The qPCR was run using PCR Sybr Green Master Mix (Roche Applied Science, Indianapolis, IN) and magnesium chloride in the Light Cycler (Roche Applied Science, Indianapolis, IN). The reaction conditions and analysis employed in the quantification of mRNA level by qPCR were performed as previously described by our laboratory [15]. The results were normalized by dividing number of copies of target mRNA by number of copies of GAPDH mRNA for each sample.

2.5. Immunocytochemistry

Neonatal cardiac myocytes were plated on glass coverslips and fixed with 70% ethanol for 20 min at −20 °C. In short, cells were first incubated for 30 min at room temperature with 2% IgG-free bovine serum albumin (BSA) to reduce nonspecific binding. This was followed by incubation with either polyclonal anti-rabbit antibody for laminin (Sigma Chemicals, L9393, diluted 1:50) or for cadherin (Sigma Chemicals, C3678, diluted 1:100) for 1 h at room temperature. For laminin and cadherin detection the cells were incubated for 1 h at room temperature with a goat anti-rabbit secondary antibody (Molecular Probes, A11008, diluted 1:400) conjugated to Alexa 488 or to Cy3 (Sigma Chemicals, 70202, diluted 1:800) respectively. The coverslips were then washed four times for 10 min each with PBS and mounted in medium for fluorescence VECTASHIELD® H-1000 (Vector Laboratories, Inc. Burlingame, CA). Fluorescence was observed on a Zeiss Axi-overt 200 M microscope (Carl Zeiss, Oberkochen, Germany).

The nuclei of the cardiac myocytes and parasites were labeled with DAPI (Sigma Chemicals; diluted 1:10000) for 5 min at 37 °C. The specificity of the immunofluorescent staining was

assessed for each experimental condition by performing the reaction in the absence of primary antibodies. No staining was observed under such conditions.

3. Results and discussion

Data complying with the "**M**inimum **I**nformation **A**bout **M**icroarray **E**xperiments" (MIAME) were deposited as GSE17330 in the National Center for Biotechnology Information Gene Expression Omnibus database (http://www.ncbi.nlm.nih.gov/geo/query/acc.cgi?acc=GSE17330). In total, 7624 non-redundant, well annotated genes were adequately quantified on all eight samples after each redundancy group was reduced to one weighted value. Of these, 420 (5.5%) were substantially different (>1.5 fold up or down-regulated) when comparing control and *T. cruzi* infected myocyte cultures. A selection of 80 up and 80 down-regulated genes is presented in Table 1. Among the immune response genes, chemokine (C-C motif) ligand 5 (*Ccl5*), chemokine (C-X-C motif) ligand 10 (*Cxcl10*), guanylate nucleotide binding protein 2 (*Gbp2*), interferon-induced with helicase C domain 1 (*Ifih1*), proteosome (prosome, macropain) subunit, beta type 8 (*Psmb8*) and receptor (TNFRSF)-interacting serine–threonine kinase 2 (*Ripk2*) were found as up-regulated. Other immune response genes such are: complement component 1, q subcomponent, alpha polypeptide (*C1qa*) and NK2 transcription factor related, locus 3 (*Nkx2-3*) were found as down-regulated. Down-regulation of matrix metalloprotease 12 (*Mmp12)* and aquaporin-1 (*Aqp1)*, and up-regulation of bone marrow stromal cell antigen 2 (*Bst2)* and profilin-1 (*Pfn1)* were validated by qRT-PCR as illustrated in Fig. 1.

In order to identify pathways differentially up- or down-regulated in the cardiac myocytes as a consequence of *T. cruzi* infection, we applied the program GenMAPP to the dataset (Gladstone Institute: http://www.genmapp.org/). Gene Ontology (GO) terms with highest Z scores ($p < 0.05$) are listed in Table 2 for both up- and down-regulated genes. Among the pathways most affected in the list of up-regulated genes in the infected myocytes were those involved in enzymatic activity (in particular, scavenger receptor, exonucleases, proteases and caspases), immune, defense and stress responses, apoptosis and activation of the proteasome, and calcium-activated potassium channel activity. Down-regulated pathways included calcium and second messenger signaling, cytoskeleton elements (actin filaments, stress fibers, myosin), enzymatic degradation (lysozyme, trypsin, metallopeptidases) and extracellular matrix. Genes regulated within each of these pathways, and possible implications of these regulations, are considered below.

3.1. Immune response genes represent a major altered pathway in infected myocytes

Virtually all immune response genes represented on the arrays were regulated in the infected myocytes. The leukocyte chemokine *Cxcl12* (also termed stromal cell-derived factor-1, *Sdf*1) was down-regulated, while *Cxcl16* (which functions as scavenger receptor in macrophages and is a powerful chemoattractant for T cells) as well as *Ccl7*, *Cxcl1* and *Cxcl16* were up-regulated. Also up-regulated were: histocompatibility 2, T region locus 10 (*H2-T10*) and interferon-induced protein with tetratricopeptide repeats 3 (*Ifit3*),. In previous microarray experiments by others and us on hearts of *T. cruzi* infected mice [7–9], similar immune response genes were found to be a major transcriptomic consequence of the infection. Strikingly, results of the present study provide evidence for autonomous activation of these pathways in the cardiac myocytes per se, implying a concerted action of immune cells infiltrating the heart and the infected myocytes themselves.

3.2. Regulated genes in other over-represented pathways

Down-regulated genes related to apoptosis included the apoptosis inhibitory proteins *Birc1b* (−3.4x) and *Birc5* (−2.8x), and up-regulated genes included the possible tumor suppressor

Axud1, the initiation factor *Eif5a*, as well as the histocompatibility complex genes listed above. Down-regulated calcium mediated signaling genes included those encoding the calcium binding protein calmodulin (*Cam1*); and the *calcineurin* interacting proteins *Dscr1* and *Dscr1l1*. Down-regulated ion channel/transporter genes included those encoding the gap junction protein Cx45 (*Gjc1*), the water channel aquaporin-1 (*Aqp1)*, and the high affinity aspartate/glutamate transporter (*Slc1A6*). Up-regulated genes in this category included the large conductance potassium channel (Kcnmb1) and the sodium/bile acid co-transporter (*Slc10a2*). Down-regulated cytoskeleton genes included the thick filament gene *Myh11* and the myosin light chain (*Myl2*), the Z-disc protein junctophilin (*Jph2*), the actin binding protein anillin (*Anln*).

3.3. Cardiac myocyte infection affects expression of extracellular matrix components

Down-regulated extracellular matrix genes included the matrix metalloproteinases *Adamts5*, *Mmp12*, and *Mmp23*, elastin (*Eln*), the metalloprotease inhibitor *Timp3*, the complement component *C1ga*, the collagens *Col4a2* and *Col6a*1, cathepsin S (*Ctss*), the chemokine *Cxcl12*, the immunosuppressive molecule *Fkbp7*, laminin-γ-1 (*Lamc1*), lysozyme (*Lyzs*) and its precursor *Lzp-s*, the microfibril associated protein *Mfap4*, the collagenase protease enhancer *Pcolce2*, the transmembrane glycoprotein *Pmp22*, the serine protease *Prss11*, prosaposin (*Psap)* and the component of elastic fibers fibulin 5 (*Fbln5*). Up-regulated genes included *H2-B1*, *H2-T23*, the macrophage lectin binding protein *Lgals3* bp, the metalloprotease inhibitor (*Timp1)*, and the protein C receptor *Procr*.

The matrix metalloproteinases (*Mmp*s) belong to a family of zinc- and calcium-dependent proteases responsible for the degradation of the extracellular matrix proteins. Concomitantly they can degrade virtually all components of the extracellular matrix [15]. Their action is counterbalanced by the tissue inhibitor matrix metalloproteinases (*Timps*) [16]. Together they play a major role in tissue remodeling processes, including cardiac remodeling [17]. In our present study we found a down-regulation of the *Mmp12* gene, which is associated with degradation of elastin and basement membrane, and an increased expression of *Timp1*. The ADAM (A disintegrin and metalloprotease) family of transmembrane proteases displays diverse functions. *ADAM* with thrombospondin-like motifs (*Adamts)* is a secreted protease characterized by thrombospondin (*TS)* motifs in their C-terminal domain [18]. During acute inflammatory states the decreased expression of both *Adamst5* and *Timp3* mRNA have been reported [19]. This is consistent with our data (both *Timp3* and *Adamst5* genes were down-regulated by 4.6 and −13.2 fold, respectively).

The ability of *T. cruzi* to degrade proteins of the extracellular matrix and the blockade of the expression of its components at the transcriptional level is critical for the establishment of the host infection. We observed this degradation of extracellular matrix protein in immunofluorescence experiments using an anti-Laminin antibody (Fig. 2D,E and F). A previous report identified an increased expression of laminin modulated by the parasite transialidase, *gp83* [20]. These authors reported that silencing of the *laminin gamma 1* gene blocked *T. cruzi* infection. Our finding of laminin gamma 1 decreased expression in infected myocyte cultures is therefore highly significant, since it suggests a paracrine defense response of the infected cardiomyocytes. The labeling for this protein disappears in infected cells when *T. cruzi* penetrates host cells by an active process [21] in a unique endocytosis fashion which involves disruption of host cell actin filaments and recruitment and fusion with lysozomes [22]. Our data show a down-regulation (6.2 fold) of the *Ctss* gene which encodes cathepsin, a lysozomal cysteine proteinase that may participate in the degradation of antigenic proteins for presentation on MHC class II molecule [23]. This may facilitate the evasion of the protozoan from the parasitophorous vacuole into the cytoplasm.

3.4. Alterations in junction-associated genes

Our previous data demonstrated that cell-cell communication through Cx43 gap junction channels virtually disappears 48 h after *T. cruzi* infection in primary myocyte cultures [24–26]. As confirmed by the present study, in which the encoding gene *Gja1* was down-regulated by 2.8 fold, at longer times of infection Cx43 levels decline [27]. The decreased intercellular coupling in the infected myocytes raises the question of whether altered expression of genes representing other components of junctional communication might be responsible for this functional alteration.

The present study demonstrates that at 48 h after infection of cultured cardiac myocytes, there is about 3 fold repression of the gene *Gjc1* encoding another gap junction protein (Cx45, a major component of gap junctions in the cardiac conduction system) and of two other genes encoding cell junction proteins: cadherin 11 (*Cdh11*) and junctophilin 2 (*Jph2*). Alteration of *Cdh11* was confirmed in immunofluorescence experiments, where infected neonatal cardiac myocytes demonstrated a dramatic reduction in expression of cadherin (Fig. 3D, E and F). Cadherins represent a major transmembrane component of adherens junctions and junctophilins represent a class of transmembrane proteins that participate in the macromolecular plasma membrane/sarcoplasmic reticulum junctional complex. Thus, cadherin or junctophilin expression might influence the degree of coupling and gap junction formation between cardiac myocytes. In addition, there may be downstream effects as a result of this altered expression. For example, *RhoA* expression was found to be 2.4x down-regulated in infected myocytes, consistent with its regulation by cadherin; because altering *RhoA* signaling may alter cardiac rhythm and conduction [28], this expression may play a role in altered cardiac electrical activity in the chagasic heart.

Plectin 1 (*Plec1*) was also found to be up-regulated, which may be of interest because of the role of this molecule in inter-linking intermediate filaments with microtubules and microfilaments, anchoring intermediate filaments to the plasma membrane and its presence in hemidesmosome multiprotein complexes that facilitate adhesion of epithelia to the basement membrane, thereby providing linkage of the intra-cellular keratin filaments to the laminins of the extracellular matrix [32].

There is increasing recognition that the intercalated disk between cardiac myocytes represents a site of both mechanical and electrical coupling [29,30]. Mouse models and human genetic mutations targeting membrane-spanning components of the intercalated disk result in cardiopathic phenotypes, as do those targeting molecules linking the junctional molecules to the cytoskeleton and even to the cytoskeleton itself [31]. Regulation of genes encoding these junctional proteins in the infected cardiac myocytes likely alters both the electrical transmission between the cells and the mechanical coupling required for optimal contraction of the heart.

The pathogenesis of chagasic heart disease represents interplay of many host factors. There are contributions by fibroblasts, the cells of the vasculature and infiltrating inflammatory cells. However, our data clearly demonstrate that the cardiac myocyte *per se* also contributes to the remodeling process even in the absence of other confounding factors.

Acknowledgments

Support was from National Institutes of Health (HL-73732, HD-32573, AI-076248, AI-052739); CAPES; CNPq and FAPERJ. RCSG, LLS and FSAF were supported by a Fogarty International Training Grant D43TW007129

References

1. Tanowitz HB, Machado FS, Jelicks LA, Shirani J, Campos de Carvalho AC, Spray DC, Factor SM, Kirchoff LV, Weiss LM. Perspectives on *Trypanosoma cruzi*-induced heart disease (Chagas disease). Prog Cardiovasc Dis 2009;51:524–539. [PubMed: 19410685]
2. Tanowitz HB, Huang H, Jelicks LA, Chandra M, Loredo ML, Weiss LM, Factor SM, Shtutin V, Mukherjee S, Kitsis RN, Christ GJ, Wittner M, Shirani J, Kisanuki YY, Yanagisawa M. Role of endothelin 1 in the pathogenesis of chronic chagasic heart disease. Infect Immun 2005;73:2496–503. [PubMed: 15784596]
3. Burleigh BA, Andrews NW. Signaling and host cell invasion by *Trypanosoma cruzi*. Curr Opin Microbiol 1998;1:461–465. [PubMed: 10066513]
4. Morris SA, Bilezikian JP, Hatcher V, Weiss LM, Tanowitz HB, Wittner M. *Trypanosoma cruzi*: infection of cultured human endothelial cells alters inositol phosphate synthesis. Exp Parasitol 1989;69:330–339. [PubMed: 2509235]
5. Vaena de Avalos S, Blader IJ, Fisher M, Boothroyd JC, Burleigh BA. Immediate/early response to *Trypanosoma cruzi* infection involves minimal modulation of host cell transcription. J Biol Chem 2002;277:639–644. [PubMed: 11668183]
6. Shigihara T, Hashimoto M, Shindo N, Aoki T. Transcriptome profile of *Trypanosoma cruzi*-infected cells: simultaneous up- and down-regulation of proliferation inhibitors and promoters. Parasitol Res 2008;102:715–722. [PubMed: 18058129]
7. Mukherjee S, Belbin TJ, Spray DC, Iacobas DA, Weiss LM, Kitsis RN, Wittner M, Jelicks LA, Scherer PE, Ding A, Tanowitz HB. Microarray analysis of changes in gene expression in a murine model of chronic chagasic cardiomyopathy. Parasitol Res 2003;91:187–196. [PubMed: 12910413]
8. Mukherjee S, Nagajyothi F, Mukhopadhyay A, Machado FS, Belbin TJ, Campos de Carvalho A, Guan F, Albanese C, Jelicks LA, Lisanti MP, Silva JS, Spray DC, Weiss LM, Tanowitz HB. Alterations in myocardial gene expression associated with experimental *Trypanosoma cruzi* infection. Genomics 2008;91:423–432. [PubMed: 18343633]
9. Garg N, Popov VL, Papaconstantinou J. Profiling gene transcription reveals a deficiency of mitochondrial oxidative phosphorylation in *Trypanosoma cruzi*-infected murine hearts: implications in chagasic myocarditis development. Biochim Biophys Acta 2003;14:106–120. [PubMed: 12853116]
10. Cunha-Neto E, Dzau VJ, Allen PD, Stamatiou D, Benvenutti L, Higuchi ML, Koyama NS, Silva JS, Kalil J, Liew CC. Cardiac gene expression profiling provides evidence for cytokinopathy as a molecular mechanism in Chagas' disease cardiomyopathy. Am J Pathol 2005;167:305–313. [PubMed: 16049318]
11. Rowin KS, Tanowitz HB, Wittner M, Nguyen HT, Nadal-Ginard B. Inhibition of muscle differentiation by *Trypanosoma cruzi*. Proc Nat Acad Sci USA 1983;80:6390–6394. [PubMed: 6413976]
12. Tanowitz HB, Wittner M, Kress Y, Bloom BR. Studies of in vitro infection by *Trypanosoma cruzi*. Am J Med Hyg 1975;24:25–33.
13. Iacobas DA, Fan C, Iacobas S, Spray DC, Haddad GG. Transcriptomic changes in developing kidney exposed to chronic hypoxia. Biochem Biophys Res Comm 2006;349(1):329–338. [PubMed: 16934745]
14. Iacobas DA, Iacobas S, Li WEI, Zoidl G, Dermietzel R, Spray DC. Genes controlling multiple functionalpathways are transcriptionally regulated in Connexin43 null mouse heart. Physiol Genomics 2005;20:211–223. [PubMed: 15585606]
15. Combs TP, Nagajyothi, Mukherjee S, de Almeida CJ, Jelicks LA, Schubert W, Lin Y, Jayabalan DS, Zhao D, Braunstein VL, Landskroner-Eiger S, Cordero A, Factor SM, Weiss LM, Lisanti MP, Tanowitz HB, Scherer PE. The adipocyte as an important target cell for *Trypanosoma cruzi* infection. J Biol Chem 2005;280:24085–24094. [PubMed: 15843370]
16. Shapiro SD, Senior RM. Matrix metalloproteinases. Matrix degradation and more. Am J Respir Cell Mol Biol 1999;20:1100–1102. [PubMed: 10340927]
17. Vicenti MP. The matrix metalloproteinase (MMP) and tissue inhibitor of metalloproteinase (TIMP) genes. Transcriptional and post-transcriptional regulation, signal transduction and cell-type-specific expression. Methods Mol Biol 2001;151:121–148. [PubMed: 11217296]

18. Spinale FG. Matrix metalloproteinases: regulation and dysregulation in the failing heart. Circ Res 2002;90:520–530. [PubMed: 11909815]
19. Porter S, Clark IM, Kevorkian L, Edwards DR. The ADAMTS metalloproteinases. Biochem J 2005;386(Pt 1):15–27. [PubMed: 15554875]
20. Cross AK, Haddock G, Surr J, Plumb J, Bunning RA, Buttle DJ, Woodroofe MN. Differential expression of ADAMTS-1, -4, -5 and TIMP-3 in rat spinal cord at different stages of acute experimental autoimmune encephalomyelitis. J Autoimmun 2006;26(1):16–23. [PubMed: 16303287]
21. Nde PN, Simmons KJ, Kleshchenko YY, Pratap S, Lima MF, Villatta F. Stable RNA interference of host thrombospondini blocks *Trypanosome cruzi* infection. Febs Lett 2006;580:2365–2370. [PubMed: 16616140]
22. Schenkman S, Robbins ES, Nussenzweig V. Attachment of *Trypanosoma cruzi* to mammalian cells requires parasite energy, and invasion can be independent of the target cell cytoskeleton. Infect Immun 1991;59:645–654. [PubMed: 1987081]
23. Tardieux I, Webster P, Ravesloot J, Boron W, Lunn JA, Heuser JE, Andrews NW. Lysosome recruitment and fusion are early events required for trypanosome invasion of mammalian cells. Cell 1992;71:1117–1130. [PubMed: 1473148]
24. Ljunggren A, Redzynia I, Alvarez-Fernandez M, Abrahamson M, Mort JS, Krupa JC, Jaskolski M, Bujacz G. Crystal structure of the parasite protease inhibitor chagasin in complex with a host target cysteine protease. J Mol Biol 2007;371:137–153. [PubMed: 17561110]
25. Campos de Carvalho AC, Tanowitz HB, Dermietzel R, Roy C, Hertzberg EL, Spray DC. Gap junction distribution is altered between cardiac myocytes infected with *Trypanosoma cruzi*. Circ Res 1992;70:733–742. [PubMed: 1551199]
26. Campos de Carvalho AC, Masuda MO, Tanowitz H, Wittner M, Goldenberg RCS, Spray DC. Conduction defects and arrhythmias in Chagas' disease: possible role of gap junctions and auto-immune mechanisms. J Cardiovasc Electrophysiol 1994;5:686–698. [PubMed: 7804521]
27. Goldenberg RCS, Gonçalves A, Campos de Carvalho AC. Gap junctions are specifically disrupted by *Trypanosoma cruzi* infection. Camilo Perachia (Org) Gap Junctions 2000;49:625–34.
28. Adesse D, Garzoni LR, Huang H, Tanowitz HB, Meirelles MN, Spray DC. *Trypanosoma cruzi* induces changes in cardiac connexin43 expression. Microbes Infect 2008;10:21–28. [PubMed: 18068391]
29. Wei L, Taffet GE, Khoury DS, Bo J, Li Y, Yatani A, Delaughter MC, Klevitsky R, Hewett TE, Robbins J, Michael LH, Schneider MD, Entman ML, Schwartz RJ. Disruption of Rho signaling results in progressive atrioventricular conduction defects while ventricular function remains preserved. FASEB J 2004;18:857–859. [PubMed: 15033930]
30. Spray DC, Duffy HS, Scemes E. Gap junctions in glia: types, roles, and plasticity. Adv Exp Med Biol 1999;468:339–359. [PubMed: 10635041]
31. Saffitz JE. Adhesion molecules: why they are important to the electrophysiologist. J Cardiovasc Electrophysiol 2006;17:225–229. [PubMed: 16533266]
32. Spray DC, Tanowitz HB. Pathology of mechanical and gap junctional co-coupling at the intercalated disc: is sepsis a junctionopathy? Crit Care Med 2007;35:2176–2185. [PubMed: 17855834]

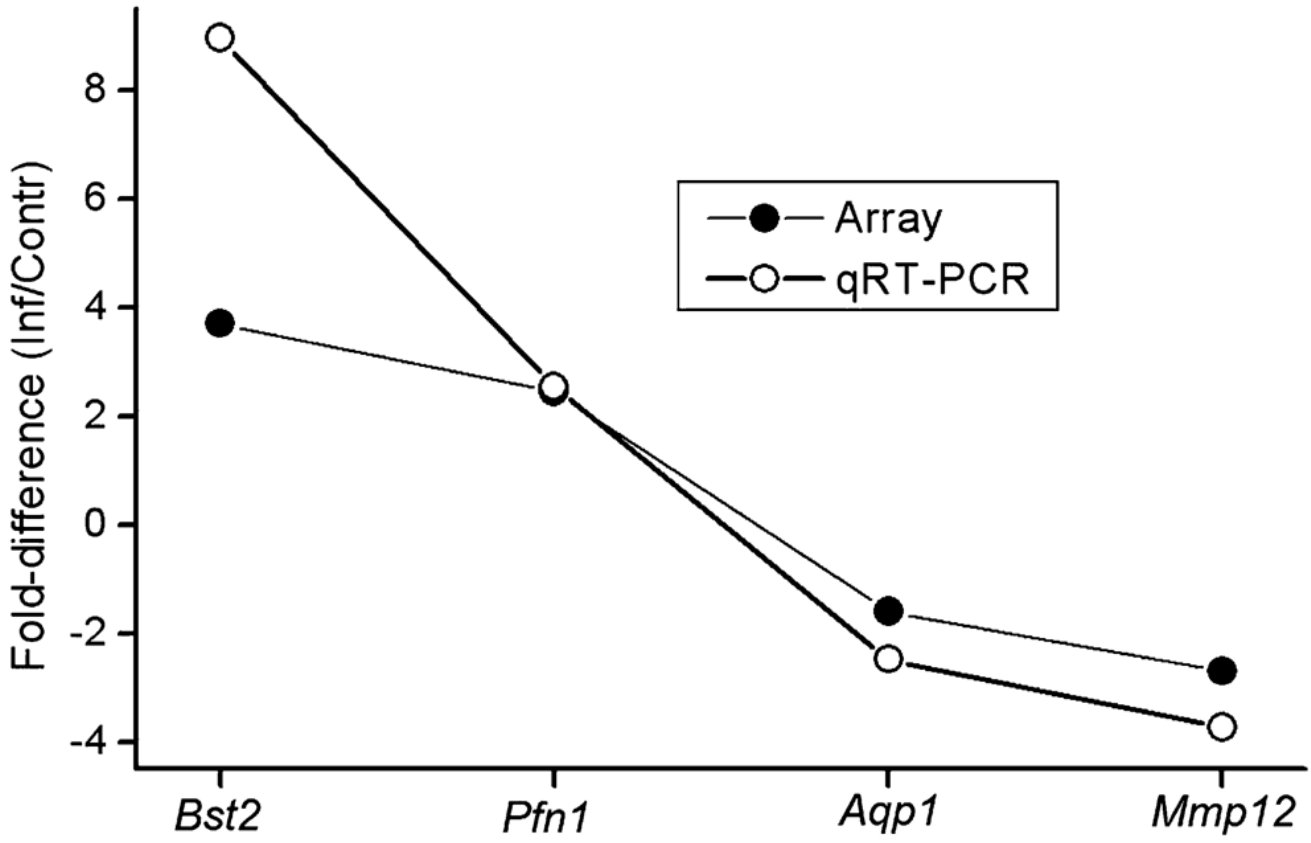

Fig. 1.

Real-time PCR validation of expression changes in four genes that were found to be altered in microarray analysis (Mmp12, Aqp1, Pfn, Bst2). Fold changes as determined by each method for each gene indicate that expression changes determined by each method are positively correlated for these sampled genes.

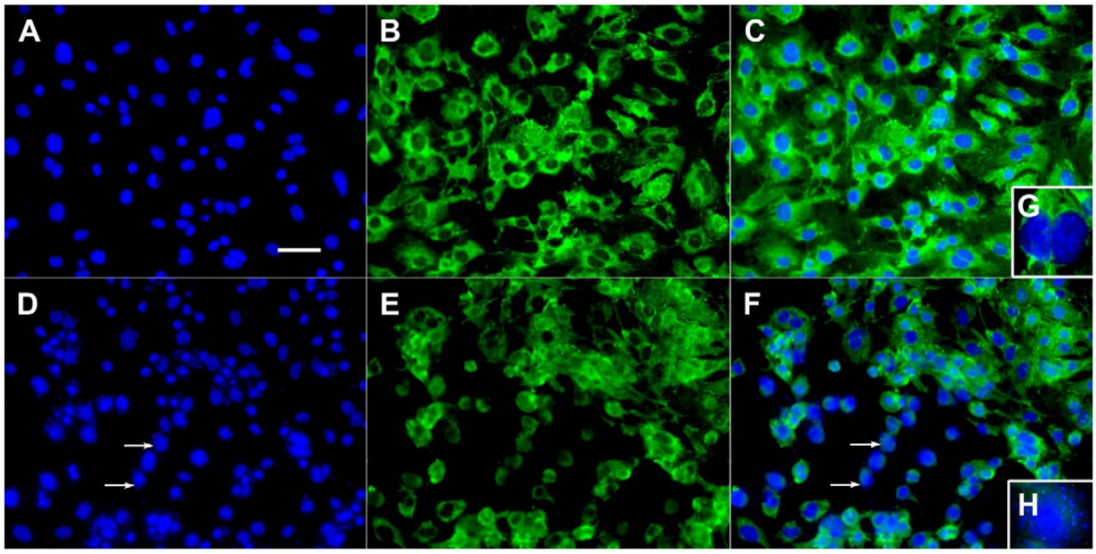

Fig. 2.

Spatial distribution of laminin in control (A–C) and *T. cruzi*-infected (D-F) neonatal cardiac myocytes. A,D: DAPI labeling; B,E: anti-laminin immunofluorescence; C, F: Merged micrographs. Note that laminin labeling is dramatically reduced in cardiac myocytes infected with the parasites (arrows in D and F). This reduction in immunolabeling is highlighted in the insets of the marked areas in C and F (G and H), where the presence of the parasites can be identified by the DAPI label (H). Bar in A: 50 μm.

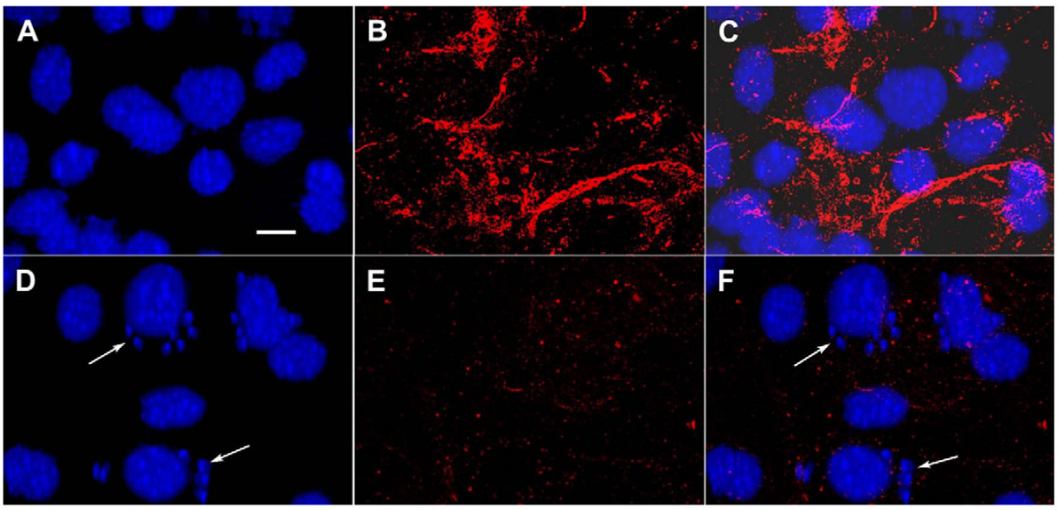

Fig. 3.
Spatial distribution of cadherin in control (A-C) and *T. cruzi*-infected (D-F) neonatal cardiac myocytes. A,D: DAPI labeling, B, E: anti-cadherin immunofluorescence; C, F: merged micrographs. Note that Cadherin labeling is dramatically reduced in cardiac myocytes infected with parasite (arrows in D and F). Bar in A: 20 μm.

Table 1

Examples of significantly up- and down-regulated genes in acutely *T. cruzi* infected cardiomyocytes (CHR = chromosomal location, X = fold-change). Note that the regulated genes are distributed in all chromosomes.

GB_ACC	Gene	SYMBOL	CHR	X
Up-regulated genes				
NM_145209	2′-5′ oligoadenylate synthetase-like 1	Oasl1	5	10.29
NM_009671	Ankyrin repeat and FYVE domain containing 1	Ankfy1	11	2.07
XM_128064	Apolipoprotein L 9a	Apol9a	15	4.12
NM_181406	Arginyl-tRNA synthetase-like	Rarsl	4	2.20
NM_153287	AXIN1 up-regulated 1	Axud1	9	2.06
NM_016767	Basic leucine zipper transcription factor, ATF-like	Batf	12	2.38
NM_175277	BolA-like 3 (*Escherichia coli*)	Bola3	6	2.50
NM_198095	Bone marrow stromal cell antigen 2	Bst2	8	7.68
NM_013653	Chemokine (C-C motif) ligand 5	Ccl5	11	58.56
NM_013654	Chemokine (C-C motif) ligand 7	Ccl7	11	4.55
NM_008176	Chemokine (C-X-C motif) ligand 1	Cxcl1	5	19.82
NM_021274	Chemokine (C-X-C motif) ligand 10	Cxcl10	5	14.91
NM_023158	Chemokine (C-X-C motif) ligand 16	Cxcl16	11	1.59
NM_029295	Chemokine-like factor	Cklf	8	1.78
NM_026036	Chemokine-like factor super family 6	Cklfsf6	9	1.65
NM_029635	COMM domain containing 9	Commd9	2	2.18
NM_028798	Cysteine-rich C-terminal 1	Crct1	3	3.62
AF151637	Cysteine-rich PDZ-binding protein	Cript	17	2.28
XM_220603	Dynein-like protein 2	DLP2	10	1.97
NM_010119	EH-domain containing 1	Ehd1	19	2.68
NM_010106	Eukaryotic translation elongation factor-1 alpha 1	Eef1a1	19	1.71
NM_181582	Eukaryotic translation initiation factor 5A	Eif5a	11	1.47
NM_016696	Glypican 1	Gpc1	1	2.17
NM_025332	GTP-binding protein 8	Gtpbp8	16	2.30
NM_010260	Guanylate nucleotide binding protein 2	Gbp2	3	2.91
NM_010395	Histocompatibility 2, T region locus 10	H2-T10	17	7.34
NM_153571	HscB iron–sulfur cluster co-chaperone homolog (*Escherichia coli*)	Hscb	5	5.57
NM_027835	Interferon-induced with helicase C domain 1	Ifih1	2	3.05
NM_008331	Interferon-induced protein with tetratricopeptide repeats 1	Ifit1	19	3.05
NM_010501	Interferon-induced protein with tetratricopeptide repeats 3	Ifit3	19	3.60
NM_133990	Interleukin 13 receptor, alpha 1	Il13ra1	X	1.65
NM_011150	Lectin, galactoside-binding, soluble, 3 binding protein	Lgals3 bp	11	2.40
XM_129166	Melan-A	Mlana	19	2.16
NM_010398	MHC class Ib antigen Qa-1 (H2-T23)	H2-D1	17	4.06
NM_008329	Myeloid cell nuclear differentiation antigen	Ifi204	1	4.92
NM_029688	Neoplastic progression 3	Npn3	2	2.18
NM_008675	Neuroblastoma, suppression of tumorigenicity 1	Nbl1	4	2.02

GB_ACC	Gene	SYMBOL	CHR	X
NM_019401	N-myc (and STAT) interactor	Nmi	2	2.03
NM_010881	Nuclear receptor coactivator 1	Ncoa1	12	6.85
XM_484255	Nucleolar protein 8	Nol8	13	1.93
NM_170591	Nucleoporin like 1	Nupl1	14	2.98
NM_207138	Olfactory receptor 149	Olfr149	9	43.86
NM_172116	Parkinson disease 7 domain containing 1	Pddc1	7	7.60
NM_011065	Period homolog 1 (*Drosophila*)	Per1	11	2.35
AF188007	Plectin 1	Plec1	15	2.06
NM_181402	Poly (ADP-ribose) polymerase family, member 11	Parp11	6	2.31
XM_488522	Poly (ADP-ribose) polymerase family, member 14	Parp14	16	3.65
NM_146169	Poly(A) binding protein interacting protein 2B	Paip2b	6	5.87
NM_025901	Polymerase (RNA) III (DNA directed) polypeptide K	Polr3 k	2	2.64
NM_027869	Polyribonucleotide nucleotidyltransferase 1	Pnpt1	11	2.23
NM_031169	Potassium large conductance calcium-activated channel, subfamily M, beta member 1	Kcnmb1	11	1.59
XM_131437	Pregnancy-associated plasma protein A	Pappa	4	7.59
NM_009439	Proteasome (prosome, macropain) 26S subunit, non-ATPase, 3	Psmd3	11	2.92
NM_011171	Protein C receptor, endothelial	Procr	2	1.59
NM_010724	Proteosome (prosome, macropain) subunit, beta type 8 (large multifunctional protease 7)	Psmb8	17	5.32
XM_205287	Protocadherin 19	Pcdh19	X	1.73
NM_021384	Radical S-adenosyl methionine domain containing 2	Rsad2	12	10.10
NM_145495	Ras and Rab interactor 1	Rin1	19	1.94
NM_138952	Receptor (TNFRSF)-interacting serine-threonine kinase 2	Ripk2	4	1.98
XM_132528	Replication factor C (activator 1) 3	Rfc3	5	2.19
NM_008487	Rho/rac guanine nucleotide exchange factor (GEF) 2	Arhgef2	3	3.02
NM_178164	ROD1 regulator of differentiation 1 (*Schizosaccharomyces pombe*)	Rod1	4	1.64
NM_203507	RWD domain containing 4A	Rwdd4a	8	1.52
NM_017380	Septin 9	Sep9	11	1.74
NM_009244	Serine (or cysteine) proteinase inhibitor, clade A, member 1a	Serpina1a	12	3.78
NM_011315	Serum amyloid A 3	Saa3	7	24.95
NM_011388	Solute carrier family 10, member 2	Slc10a2	8	1.62
NM_011774	Solute carrier family 30 (zinc transporter), member 4	Slc30a4	2	1.56
BC058669	Spire homolog 1 (Drosophila)	Spire1	18	1.65
NM_011506	Succinate-Coenzyme A ligase, ADP-forming, beta subunit	Sucla2	14	3.14
AF110520	TAP binding protein	Tapbp	17;15	2.11
NM_011637	Three prime repair exonuclease 1	Trex1	9	2.95
NM_011593	Tissue inhibitor of metalloproteinase 1	Timp1	X	1.95
BC071216	Torsin family 3, member A	Tor3a	1	3.99
NM_009099	Tripartite motif protein 30	Trim30	7	3.64
XM_148271	Ubinuclein 1	Ubn1	16	2.51
NM_011551	Upstream binding transcription factor, RNA polymerase I	Ubtf	11	1.82

GB_ACC	Gene	SYMBOL	CHR	X
NM_010757	V-maf musculoaponeurotic fibrosarcoma oncogene family, protein K (avian)	Mafk	5	2.74
NM_011683	Vomeronasal 1 receptor, A1	V1ra1	6	1.82
NM_172893	Zinc finger CCCH type domain containing 1	Zc3hdc1	6	2.79
Down-regulated genes				
NM_011782	A disintegrin-like and metalloprotease (reprolysin type) with thrombospondin type 1 motif, 5	(Adamts5)	16	−13.22
NM_007475	Acidic ribosomal phosphoprotein P0	Arbp	5	−3.82
NM_033268	Actinin alpha 2	Actn2	13	−2.75
NM_007479	ADP-ribosylation factor 4	Arf4	14	−4.17
NM_028390	Anillin, actin binding protein (scraps homolog, *Drosophila*)	Anln	9	−3.86
NM_007472	Aquaporin-1	Aqp1	6	−4.18
NM_009700	Aquaporin-4	Aqp4	18	−4.88
NM_010872	Baculoviral IAP repeat-containing 1b	Birc1b	13	−3.39
NM_009689	Baculoviral IAP repeat-containing 5	Birc5	11	−2.83
NM_018819	Brain protein 44-like	Brp44l	17	−3.86
NM_009866	Cadherin 11	Cdh11	8	−2.93
NM_007589	calmodulin 1	Calm1	17	−2.39
NM_009922	Calponin 1	Cnn1	9	−4.14
NM_013494	Carboxypeptidase E	Cpe	8	−3.36
NM_021281	Cathepsin S	Ctss	3	−6.17
NM_153098	CD109 antigen	Cd109	9	−4.32
NM_021704	Chemokine (C-X-C motif) ligand 12	Cxcl12	6	−9.69
AB075019	Coiled-coil domain containing 80	Ccdc80	16	−5.84
NM_007572	Complement component 1, q subcomponent, alpha polypeptide	C1qa	4	−7.74
NM_026082	Dedicator of cytokinesis 7	Dock7	4	−3.40
NM_019771	Destrin	Dstn	2	−3.48
NM_030598	Down syndrome critical region gene 1-like 1	Dscr1l1	17	−3.33
NM_019466	Down syndrome critical region homolog 1 (human)	Dscr1	16	−3.10
NM_010078	Dystrophin related protein 2	Drp2	X	−3.91
NM_007925	Elastin	Eln	5	−7.65
NM_025794	Electron transferring flavoprotein, dehydrogenase	Etfdh	3	−4.25
NM_007993	Fibrillin 1	Fbn1	2	−4.66
NM_011812	Fibulin 5	Fbln5	12	−3.53
NM_010222	FK506 binding protein 7	Fkbp7	2	−4.31
NM_008046	Follistatin	Fst	13	−6.07
NM_010288	Gap junction membrane channel protein alpha 1	Gja1	10	−2.77
NM_008122	Gap junction membrane channel protein gamma 1	Gjc1	11	−3.22
NM_008409	Integral membrane protein 2A	Itm2a	X	−5.02
NM_00100130	In9tegrin alpha 8	Itga8	2	−5.38
NM_028007	Integrin alpha FG-GAP repeat containing 1	Itfg1	8	−3.92
NM_021566	Junctophilin 2	Jph2	2	−3.36
NM_010683	Laminin, gamma 1	Lamc1	1	−3.27

GB_ACC	Gene	SYMBOL	CHR	X
NM_017372	Lysozyme	Lyzs	10	−6.27
NM_019499	MAD2 (mitotic arrest deficient, homolog)-like 1 (yeast)	Mad2l1	6	−3.57
NM_008618	Malate dehydrogenase 1, NAD (soluble)	Mdh1	11	−3.99
NM_008605	Matrix metalloproteinase 12	Mmp12	9	−6.73
NM_011985	Matrix metalloproteinase 23	Mmp23	4	−4.20
XM_133510	Methylmalonyl CoA epimerase	Mcee	7	−3.38
NM_029568	Microfibrillar-associated protein 4	Mfap4	11	−8.82
NM_008622	Mpv17 transgene, kidney disease mutant	Mpv17	5	−4.21
NM_175260	Myosin heavy chain 10, non-muscle	Myh10	11	−3.92
NM_013607	Myosin, heavy polypeptide 11, smooth muscle	Myh11	16	−1.86
NM_010861	Myosin, light polypeptide 2, regulatory, cardiac, slow	Myl2	5	−3.87
NM_144870	NADH dehydrogenase (ubiquinone) Fe–S protein 8	Ndufs8	19	−5.04
NM_008695	Nidogen 2	Nid2	14	−4.60
NM_011615	Nitrilase 1	Nit1	1	−5.94
NM_008699	NK2 transcription factor related, locus 3 (*Drosophila*)	Nkx2-3	19	−2.46
NM_026532	Nuclear transport factor 2	Nutf2	8	−3.96
NM_020288	Olfactory receptor 749	Olfr749	14	−3.88
NM_013590	P lysozyme structural	Lzp-s	10	−17.78
NM_008885	Peripheral myelin protein	Pmp22	11	−5.42
NM_016764	Peroxiredoxin 4	Prdx4	X	−5.11
XM_242396	Polymerase (DNA directed), alpha 1	Pola1	X	−6.59
NM_027196	Polymerase (DNA-directed), delta 4	Pold4	19	−5.19
NM_021342	Potassium voltage-gated channel, Isk-related subfamily, gene 4	Kcne4	1	−3.81
NM_029620	Procollagen C-endopeptidase enhancer 2	Pcolce2	9	−3.17
NM_009932	Procollagen, type IV, alpha 2	Col4a2	8	−6.27
NM_009933	Procollagen, type VI, alpha 1	Col6a1	10	−8.80
NM_011179	Prosaposin	Psap	10	−4.57
NM_019564	Protease, serine, 11 (Igf binding)	Prss11	7	−4.19
NM_146081	Protein phosphatase 4, regulatory subunit 1	Ppp4r1	17	−3.69
NM_016802	Ras homolog gene family, member A	Rhoa	9	−2.41
NM_009200	Solute carrier family 1 (high affinity aspartate/glutamate transporter), member 6	Slc1a6	10	−3.35
NM_026255	Solute carrier family 25 (mitochondrial carrier, phosphate carrier), member 26	Slc25a26	6	−4.52
Z47775	Sorbin and SH3 domain containing 2	Sorbs2	8	−3.69
NM_025303	Staufen (RNA binding protein) homolog 2 (Drosophila)	Stau2	1	−3.95
NM_023374	Succinate dehydrogenase complex, subunit B, iron–sulfur (Ip)	Sdhb	4	−4.10
NM_029811	Suppression of tumorigenicity 5	St5	7	−3.65
AY548113	Thioredoxin domain containing 12 (endoplasmic reticulum)	Txndc12	4	−3.65
NM_172597	Thioredoxin domain containing 16	Txndc16	14	−3.45
NM_011595	Tissue inhibitor of metalloproteinase 3	Timp3	10	−4.61
NM_011626	TPA regulated locus	Tparl	5	−3.71
NM_009367	Transforming growth factor, beta 2	Tgfb2	1	−6.33

GB_ACC	Gene	SYMBOL	CHR	X
NM_016873	WNT1 inducible signaling pathway protein 2	Wisp2	2	−12.76
AF017806	Zinc finger protein 292	Zfp292	4	−4.17

Table 2

Gene ontology (GO) categories of up- and down-regulated genes with highest Z scores (C = cellular location, F = molecular function, P = biological process).

GOID	GO Name	Type	Z Score	PermuteP
Up-regulated in infected myocytes				
5044	Scavenger receptor activity	F	6.148	0
30234	Enzyme regulator activity	F	5.138	0.001
4527	Exonuclease activity	F	4.827	0.001
9891	Positive regulation of biosynthesis	P	5.906	0.002
6955	Immune response	P	4.121	0.002
6952	Defense response	P	3.788	0.002
8047	Enzyme activator activity	F	4.544	0.003
50819	Negative regulation of coagulation	P	5.906	0.006
8538	Proteasome activator activity	F	4.685	0.013
6563	L-serine metabolism	P	3.939	0.021
7249	I-kappaB kinase/NF-kappaB cascade	P	3.417	0.023
6917	Induction of apoptosis	P	2.654	0.037
16504	Protease activator activity	F	4.175	0.042
8656	Caspase activator activity	F	4.175	0.042
16505	Apoptotic protease activator activity	F	4.175	0.042
42060	Wound healing	P	3.022	0.042
51051	Negative regulation of transport	P	4.175	0.045
45806	Negative regulation of endocytosis	P	4.175	0.045
6950	Response to stress	P	2.176	0.045
15269	Calcium-activated potassium channel activity	F	4.175	0.046
4617	Phosphoglycerate dehydrogenase activity	F	4.175	0.046
4704	NF-kappaB-inducing kinase activity	F	4.175	0.047
4112	Cyclic-nucleotide phosphodiesterase activity	F	4.175	0.049
4114	3′,5′-cyclic-nucleotide phosphodiesterase activity	F	4.175	0.049
Down-regulated in infected myocytes				
19722	Calcium-mediated signaling	P	5.564	0.002
51017	Actin filament bundle formation	P	5.564	0.003
4295	Trypsin activity	F	5.564	0.003
43149	Stress fiber formation	P	5.564	0.003
3796	Lysozyme activity	F	5.564	0.005
19932	Second-messenger-mediated signaling	P	5.056	0.001
4222	Metalloendopeptidase activity	F	4.05	0.003
3845	11-beta-hydroxysteroid dehydrogenase activity	F	3.933	0.048
5859	Muscle myosin	C	3.933	0.051
31012	Extracellular matrix	C	3.914	0.002
5604	Basement membrane	C	3.433	0.014
4175	Endopeptidase activity	F	3.253	0.002
5576	Extracellular region	C	3.196	0.003

GOID	GO Name	Type	Z Score	PermuteP
7519	Myogenesis	P	3.181	0.025
4984	Olfactory receptor activity	F	3.181	0.028
7015	Actin filament organization	P	3.181	0.029
42598	Vesicular fraction	C	3.178	0.023
8237	Metallopeptidase activity	F	3.169	0.01
6817	Phosphate transport	P	2.954	0.024
30016	Myofibril	C	2.801	0.048
43292	Contractile fiber	C	2.801	0.048
30017	Sarcomere	C	2.801	0.048
7517	Muscle development	P	2.416	0.051
6508	Proteolysis and peptidolysis	P	2.247	0.026
44257	Cellular protein catabolism	P	2.247	0.026
5489	Electron transporter activity	F	2.057	0.046
8270	Zinc ion binding	F	1.991	0.048